Synthesis, structure and magnetic behavior of Potassium Birnessite

A. G. Mike Uiterwijk*

Daily supervisor: Liliia D. Kulish **First Assessor: Graeme R. Blake** **Second Assessor: Beatriz Noheda**

Zernike Institute for Advanced Materials, University of Groningen, Nijenborgh 4, 9747 AG, Groningen, The Netherlands

a.g.m.uiterwijk@student.rug.nl

Received November 27, 2019

ABSTRACT

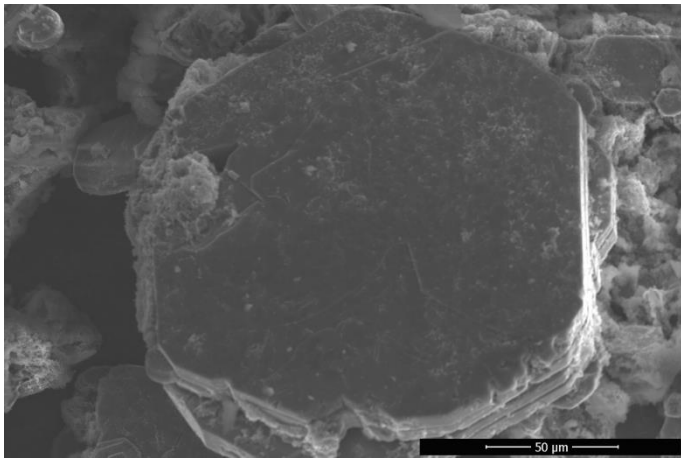

In this study potassium birnessite was attempted to be synthesized in three different methods, the latter of which proved the most successful due to the usage of an Al_2O_3 crucible. Investigation was done regarding the structure and magnetic properties that could arise from magnetic frustration of a triangular lattice. Crystals of 300µm were synthesized with hexagonal structure with space group $P6_3/mmc$. The magnetic behavior observed may be explained by the dimerised chain spin gap network.

Current research around magnetic skyrmions shows that they might present a good alternative to modern day data storage. The advantage lies in the energy required to stabilize the bits, which is much lower for skyrmions than the bit switching in electronics used nowadays[1]. Application in race-track memory storage devices has also been theorised[2]. Furthermore, their response to extermal fields hold promising applications to spintronic device functions[3,4,5]. Skyrmions are magnetic spin structures first described by Tony Skyrme in 1962[6]. Skyrmions can be classified as vortex like swirling spin solitons that are present in domain walls and magnetic bubbles. The structures which can be classified in four different quantised topological structures (*Figure 1*[7]) shows a transformation from a negative spin inside going to an opposed spin on the periphery. This property makes the skyrmions able to adapt the identity of bits which in term makes them usable as data storage.

Figure 1. (a) Hedgehog skyrmion and (b) Vortex Skyrmion. Equivalent structures with opposite spins are antiskyrmions.

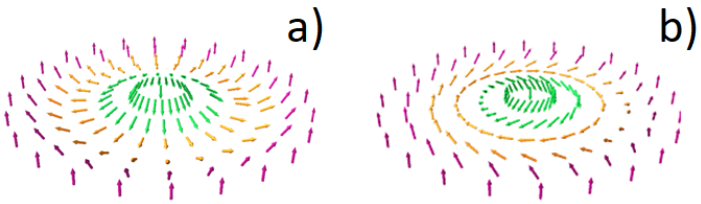

When a magnetic field is applied, the magnetisations in a skyrmion are parallel to the applied field at its periphery and antiparallel at its centre (and vice versa for antiskyrmions). The interactions and structure originate mainly from the finite Dzyaloshinskii-Moriya interaction in non centosymmetric crystals. This interaction alone favors a rotating magnetisation allignment. Ferromagnetic exchange interactions however, favors a colinear ferromagnetic spin allignment. The competition between these two interactions results in a vortex like spin with a uniform turn angle realised in the absence of an external magnetic field[8-11]. In addition to these two mechanisms, frustrated exchange interactions [12] have been proposed to be an origin for skyrmion formation. While the skyrmion crystal phase has low stability in a 3D model, they turn out to have a great stability in a 2D system[13]. The enhanced stability of skyrmions in 2D systems are realised due to the fact that when a magnetic field is applied in a 3D system, the conical order propagating wave vector and net magnetisation become stabilized. In a 2D system however, the spins can no longer rotate when a magnetic field is applied normal to the plane. The skyrmion crystal phase then gains stability against the conical state[14].

So far skyrmions have only been proven in bulk material of scales larger than 50nm[15] and in chiral-lattice magnets[16,17], but they have been theorised to also be present in so called frustrated magnets. While the temperature as well as the applied magnetic field are predicted to be larger for frustrated magnets than chiral magnets, there seem to be some other advantages to the skyrmions in a magnetically frustrated sytsem. Namely that in a frustrated magnet skyrmions and anti skymions can exist simultaneosly. Frustration is an effect most common in anti-ferromagnets. The effect occurs due to specific alignment of magnetic spins. Placing spins on a triangular lattice, the anti-ferromagnetic coupling cannot be satisfied in all directions. This causes a spin to be frustrated as shown in *Figure 2*. This is due to the competition between ferromagnetic and antiferromagnetic exchange interactions in triangular or tetrahedral crystals lattices that share corners, edges or faces[18,19]. The frustration results in a rich magnetic phase diagram with many exotic phases inluding the afore mentioned phase consisting of both types of skyrmions.

Figure 2. Depiction of magnetic frustration in a triangular lattice (a) in 2D and (b) in 3D.

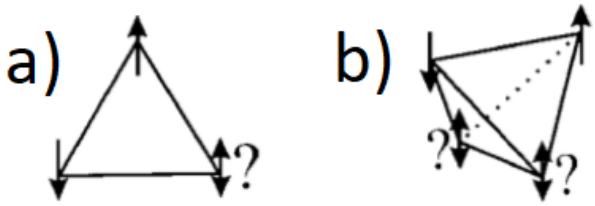

Birnessites are compounds that are described by the chemical formula $A_xMnO_2 \cdot y\ H_2O$ where A are often alkali metals (Li, Na, K, Rb, Cs) but can also be non-alkali metals such as Cu or Mg. A general consensus is attained about the fact that birnessites consist of alternating planes of manganese oxide and planes of alkali cations with water. The manganese oxide sheets are the magnetic layers that can be adjusted to alter the properties. The non-magnetic A^+-H_2O layers are able to decouple the MnO_6 layers[20] by a d-spacing by approximately 7Å[21]. The structure of the birnessite allows for a lot of tuning possibilities regarding the magnetic exchange and anisotropy along the stacking direction. Some discussion has risen concerning the existence of manganese vacancies in the manganese layers. The vacancies result from charge stabilization and are dependent on synthesis conditions. Lower pH-values

Figure 3. Structure of K-Birnessite from the crystallographic database (a) trigonal space group R-3m[23] and (b) hexagonal space group $P6_3/mmc$[24]

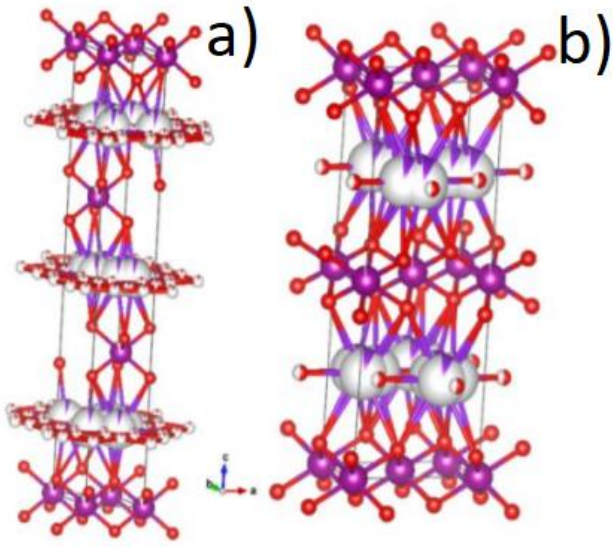

corresponds to higher amount of vacancies. However, structures synthesized at low pH have also been found consisting without vacancies[22]. The structure of birnessite differs per literature as many researchers

have attempted to solve the structure. There is a consensus that the oxygen atoms are arranged at octahedral positions to the manganese atoms in a 2D sheet, but the exact arrangement of the interlayer is not trivial. The interlayer exist out of the alkali metal atoms and water molecules but it is uncertain where their exact positions are. Most structures of birnessite are merely based on powder diffraction fits making it difficult to identify the alkali metal and water sites. This results in researchers assigning different crystal classes to birnessites due to the alkali/water distribution (*Figure 3)* Lastly, not many studies have been performed in terms of the magnetism of birnessite, especially little on potassium birnessite. Only a study about K-doped MnO_2 is found[25]. This data might not be the most accurate due to the fact that this compound does not exist of alternating layers, but it shows the closest resemblance

This thesis focuses on a specific birnessite, namely the compound with potassium. This was chosen since a synthesis method was found that supposedly would be able to synthesize potassium birnessite. Potassium birnessite was also chosen as a bit of research surrounding the compound was done before by Scholtens *et al.* [26] from our own research group. The afore mentioned d-spacing of approximately 7Å causes the birnessite to have a 2D structure. Next to that, the magnetic cations form a triangular 2D lattice allowing for magnetic frustration. The 2D magnetic frustration could case skyrmions to be formed. The large spacing and no interlayer coupling results in magnetic anisotropy and therefore it is predicted to stabilize the skyrmion phase. The potassium birnessite was attempted to be synthesized with different synthesis conditions. It has been shown that synthesis conditions are likely to result in different birnessites[22]. By attempting the synthesis following different routes, some more clarity around what causes crystals to grow to a certain form might be accomplished. To gain this information, the structure and magnetic properties of the products will be analyzed by several methods.

Research Methodology

TG-DSC analysis was done using the TG 2960 SDT. The argon flow was set to 100 ml/min with a heating rate of 10 °C/min, and samples were measured in a temperature range from 30°C-900°C.

For valence state determination, a titration method [27] was used. 0.03g of potassium birnessite was dissolved in a mixture of 5mL 0.5M sodium oxalate in water and 10mL 1.8M H_2SO_4. The manganese from the birnessite is reduced to Mn^{2+} while the oxalate is oxidezed to CO_2 and H_2O so that *Reaction 1* occurs.

$$(x-1)C_2O_4^{2-} + 2xH^+ + MnO_x \longrightarrow Mn^{2+} + (2x-2)CO_2 + xH_2O \qquad \textit{(Reaction 1)}$$

The unreacted oxalate can than be titrated back using a 0.025M $KMnO_4$ solution according to *Reaction 2.*

$$2MnO_4^- + 5H_2C_2O_4 + 6H^+ \longrightarrow 10CO_2 + 2Mn^{2+} + 8H_2O \qquad \textit{(Reaction 2)}$$

With this, the valence state of the birnessite can be determined, and together with the data of the structural water loss from the TGA-DSC analysis, the final stociometry of $K_xMnO_2 \cdot yH_2O$.

For EDS and SEM, a Fei NovaNanoSEM 650 with EDAX EDS/EBSD detectors was used for collecting data. This was analyzed with TEAM/EDS software.

The structure determination with PXRD was obtained from a Bruker d8 advance system with Cu Kα radiation (1.5418Å). Normal samples were prepared by grinding product to a fine powder where possible. Small samples made after TGA, were prepared by sticking powder with grease to a zero silicon background. Samples were measured with the θ/2θ setup and measured from 5-70° for 2θ. The obtained PXRD patterns were fitted with the GSAS-I software to obtain phase composition.The patterns were initially compared to the Potassium-Birnessite cell parameters found by Lopano *et al.*[28] with the triclinic space group C-1.

Structure was further determined by SCXRD. For this, the Bruker d8 Venture system was used with Mo Kα radiation (0.71073Å). Measurements were set to capture a full sphere for the maximal amount of unique reflections.

Magnetic properties were determined with an MPMS system. The DC susceptibility was measured by preforming a field cooled (FC) and zero field cooled (ZFC) measurement from 2K to 300K.

Synthesis of Potassium Birnessite

Single crystals of potassium birnessite ($K_xMnO_2 \cdot y H_2O$) was synthesized three times. The synthesis were adaptations to the method of Yang *et al.*[29] In the first synthesis, a 5:1 molar ratio of KNO_3 *(3.23g, 0.0317mol)* and Mn_2O_3 *(0.996g, 0.00631mol)* was mixed with 1wt% B_2O_3 *(0.040g)* and grinded. The mixture was transferred to a platinum crucible with a platinum lid and heated to 700°C over a period of 6hours. At this temperature KNO_3 decomposes to KO_2 according to *Reaction 3*.

$$2KNO_3 \longrightarrow 2KNO_2 + O_2 \longrightarrow 2KO_2 + N_2 + O_2 \qquad \textit{(Reaction 3)}$$

The KO_2 then reacts with the Mn_2O_3 to create the birnessite following *Reaction 4*:

$$4KO_2 + 2Mn_2O_3 \longrightarrow 4KMnO_2 + 3O_2 \qquad \textit{(Reaction 4)}$$

The crucible was kept in this state for 60hours after which the mixture was cooled slowly to room temperature over a period of 12hours to allow crystallization. The crystals were black and clumped together. When water was added to the sample, it turned purple, and the crucible had green traces left caused by leftover $KMnO_4$. The crystal were washed with 500ml water over a filter while constantly removing the supernatant until the supernatant turned colorless. The crystals were dried overnight at 60°C and a black powder, with small reflecting crystals remained *(Figure 4a, Potassium Birnessite (I))*. The crystals from the first synthesis were too small to be analyzed by SCXRD and MPMS.

In the second synthesis, the molar ratio of starting compounds and flux was changed from the first synthesis.

The flux was changed to contain both *(0.707g, 0.00317mol)* PbO and *(0.665g, 0.00956mol)* B_2O_3. The molar ratio was changed to 1.1:1 so that only a small excess of *(0.708g, 0.00696mol)* KNO_3 was present compared to the *(1.01g, 0.00640mol)* Mn_2O_3. In the second synthesis, the platinum crucible and lid from the first synthesis were used again. The cleaning was first done similair to the first synthesis, but when after using 1.8L H_2O the pH had only increased from 9 to 10, the black powder was put in a mixture of 250mL H_2O and 100mL HNO_3 (65%). The crystals were washed after 2 hours with 900mL water and the pH changed from 0 to 1. The product was dried overnight. After ESD showed high amount of Pb still present in the sample, the powder was again put in a mixture of of 250mL H_2O and 100mL HNO_3 (65%). After 4 hours the compound was washed with approximatily 400mL H_2O until the pH had shifted from 1 to 6 and the supernatant was colorless. The product was dried overnight at 70°C. The second synthesis showed no sign of crystal formation *(Figure 4b Potassium Birnessite (II))*, therefore this product was not analyzed by SCXRD and MPMS.

The third synthesis was very similair to the first synthesis (*3.18g, 0.0315mol* KNO_3, *1.08g, 0.00684mol* Mn_2O_3 and *0.042g* B_2O_3), however, an alumina crucible and lid was used instead of a platinum crucible. Furthermore, the crystal was washed by decanting the supernatant until it turned colorless rather than using a filter. The pH was also measured during the washing as an extra method to measure the cleansing, which changed slowly from 10 to 5, indicating the removal of all the manganese oxide with different oxidation states. The crystals obtained from the second synthesis were black crystals *(Figure 4c Potassium Birnessite (III))* and big enough to analyze with SCXRD and MPMS.

Figure 4. Products of synthesis under an optical microscope.

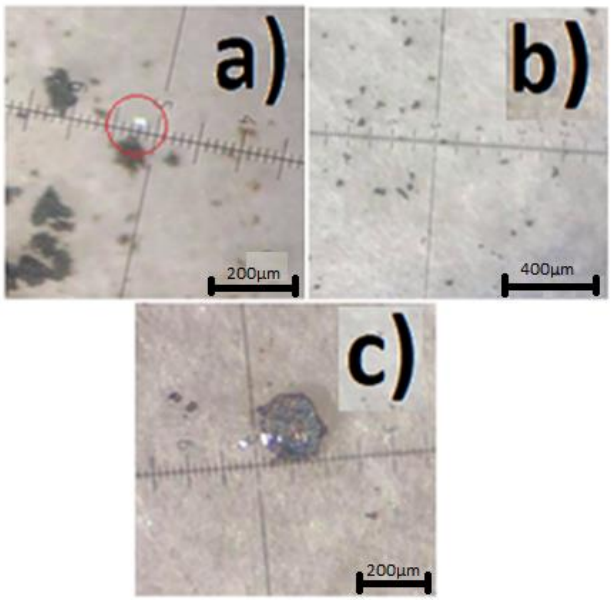

Experimental Section

Potassium Birnessite $K_{0.94}MnO_2 \cdot 0.43\ H_2O$
A 5:1 molar ratio KNO_3 *(3.18g, 0.0315mol)* and Mn_2O_3 *(1.08g, 0.00684mol)* was mixed with 1wt% *(0.042g)* B_2O_3 and grinded. The mixture was heated to 700°C in a period of 6hours. The mixture was kept in this state for 60hours in a Al crucible with Al lid. The mixture was cooled to room temperature in 12hours. The crystals were washed with water and decanted until the supernatant turned colourless.The pH was changed during washing from 10 to 5. The crystals were dried at 70°C.

Valence state determination of Potassium Birnessite
Potassium Birnessite *(0.03 g, 0.22 mmol)* was dissolved in 5 ml (0.5 M) $Na_2C_2O_4$ in H_2O and 10 mL (1.8 M) H_2SO_4. Unreacted oxylate is titrated back with a 0.025 M $KMnO_4$ solution.

Results and Discussion

Potassium Birnessite (I) during the washing of the first synthesized crystals, the filter that was used to keep the supernatant and residue seperated broke. The crystals were filtered again and some more water was used to assure that the crystals were cleaned of the flux. *Figure 4a* contains a crystal which is visible but very small. The crystal was very thin. From this we can determine the approximate dimensions of the crystal to be 40µm in length, 20µm in width and 2µm in thickness. These sizes are too small for SCXRD.

From the SEM pictures can be seen that some small crystals were formed during the synthesis. The crystals show a layers and a hexagonal structure, which was also observed by Yang *et al.*[29]. The crystals vary in size from 2-8µm. Next to the crystals, some sort of powder is also observed. This is most likely some compound that was not washed off of the crystals. The powder also consists

Figure 5. SEM picture of potassium birnessite (I) with CBS detector.

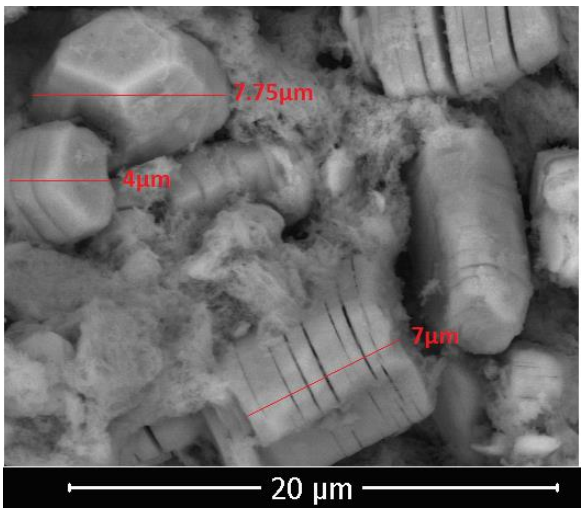

out of birnessite with similar composition as the CBS detector showed similar intensities and EDS did not show that the dust consisted of a different phase.

While the crystals were not analyzed by SCXRD, PXRD was possible for this product. *Figure 6* shows that birnessite was formed but that there was still small traces of Mn_2O_3 left in the product. This can be seen from the small characteristic peaks also being present in the diffraction pattern. It can also be observed that a single birnessite phase is present since different alkali and water contents lead to different interlayer spacing resulting in shifted 00l peaks. The powder shows a high preferred orientation in the 00l direction, which made it difficult to fit the spectrum with the right intensities. After refinement of the data, the lattice parameters of the crystals were determined to be as presented in *Table 1*.

Figure 6. (a) Powder diffraction pattern of potassium birnessite(I) fitted to triclinic C-1 space group. ◆ belongs to Mn_2O_3. (b) same diffraction pattern zoomed in on Mn_2O_3 peaks

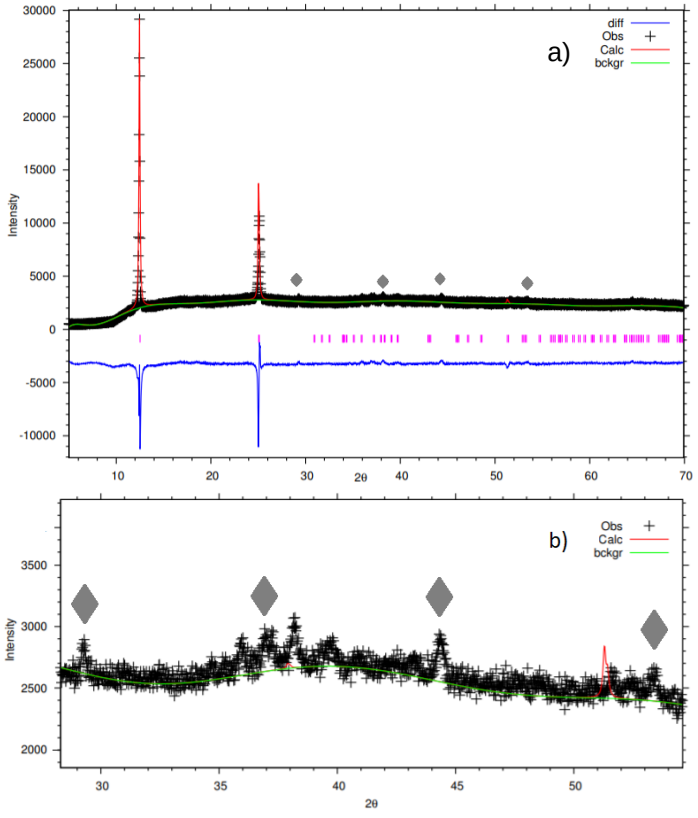

Table 1: Cell parameters after diffraction refinement.

Class	Sgr	a	b	c	α	β	γ
Triclinic	C-1	5.8(22)	3.1(14)	7.3(8)	92.(22)	104.(23)	91.(45)

To determine the stoichiometry of the birnessite, first a TG-DSC analysis was preformed *(Figure 7).* The analysis shows three endothermic effects in the sample. The first can be correlated to the loss of surface water that was still present in the sample. The mass loss was 7.55% and the curve of the time derivative of TG shows it completed at around 123.8°C with a maximum of the DSC curve at 70.5°C. The second effect correlates to the water that is embedded in the potassium birnessite structure. The total mass loss of the sample shows to be 11.87%. The derivative tells us that it was completed around 194.2°C and that there was a maximum of the DSC curve at 140.5°C. By looking at the difference in the mass losses at these points in the TG curve, we can determine the amount of water present in the birnessite. For this birnessite, the water percentage was determined to be 4.32%. This is a lower amount of water compared to prior studies of potassium birnessite[30]. The last endothermic effect that was analyzed accounts for the decomposition of birnessite into a manganese oxide. The DTG tells us this was finished at 829.3°C with a maximum in the DSC curve at 793.7°C.

Figure 7. TG-DSC analysis of potassium birnessite (I). The black and red curve (top) correspond to TG and DSC respectively, while the blue curve (bottom) represents DTG.

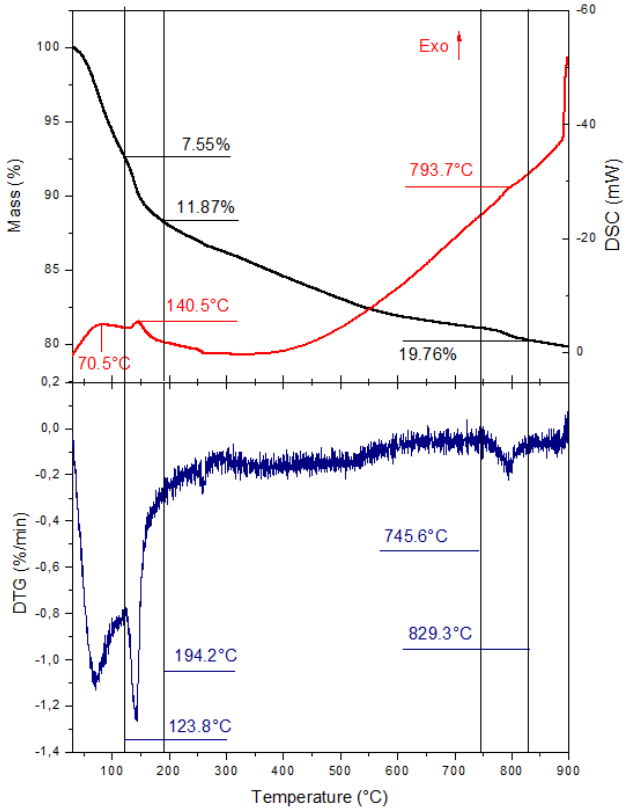

The valence state of the birnessite was also attempted to be determined with the back titration method[27]. However, after multiple attempts, too little amount of sodium oxalate was used to create a reasonable oxidation state of Mn was required. The amount of oxalate used resulted in a theoretical oxidation state of 4.6 while the allowed values were in between 3-4. Detailed calculations can be found in the appendix. Because of this, no stoichiometry value for potassium was found with this method. However, because of the failed attempt of

determining the amount of potassium in the birnessite with the valence state determination, EDS was used to give a value *(Figure 8).* From *Table 2* we can determine the amount of Potassium in the birnessite from the ratio of atomic weight percentage. EDS tells us that the K:Mn ratio is equal to 0.38. Using the calculations from the back titration method and the % of water loss determined by TGA, we can calculate the stoichiometry of the potassium birnessite to be: $K_{0.38}MnO_2 \cdot 0.25H_2O$.

One should note that EDS is not the best method to determine stoichiometry of a compound since it only measures the surface of a compound. Given the fact that potassium can also decompose from the birnessite as it can react with water still present at the surface. Thus the surface might contain less potassium than the compound. EDS probing thickness is around 10 µm and since the biggest crystals were 10µm in thickness, EDS might be able to detect the whole crystal. Because back titration failed, this can be considered as a good alternative though the actual values for K_x and $y \cdot H_2O$ might be larger then presented.

Figure 8. EDS spectrum and from *Figure 2.*

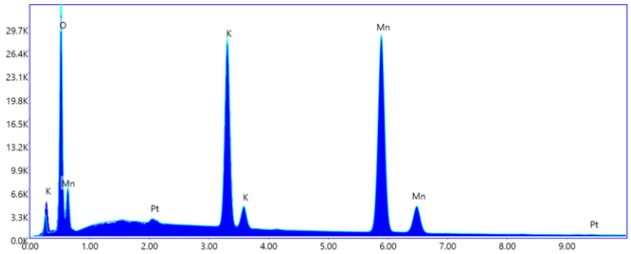

Table 2: Atomic weight percent by EDS-mapping.

Element	Wt%	At%	K_{ratio}	Z	A	F
O K	17.68	40.56	0.0813	1.2289	0.3744	1.0000
PtM	0.51	0.10	0.0045	0.7029	1.1658	1.0919
K K	17.28	16.22	0.1740	1.0338	0.9584	1.0168
MnK	64.54	43.13	0.5915	0.9225	0.9909	1.0026

Conclusion

The data collected suggests that potassium birnessite was formed with chemical formula $K_{0.38}MnO_2 \cdot 0.25H_2O$ by the first synthesis. The crystals grown were very small. EDS shows traces of Pt present in the sample, left from the crucible during the synthesis. Pt has shown to be one of the most active oxidizing metals for this process [31]. Previous studies proposed that synthesis conditions can alter the crystallization process[22]. Studies that used an Al_2O_3 crucible to synthesize birnessites have shown bigger crystals can be grown[29]. Further investigation is required to see whether this holds when longer heating times or slower cooling rates are applied as well as a different crucible. Due to time constraints, this could not be tested further.

Potassium Birnessite (II) the product from the second synthesis were first attempted to wash solely with water. However, when 1.8L water was used to wash the product, the pH had increased from 9 to 10, while the goal was to actually lower the pH to an almost neutral value. Therefore, the product was put in a mixture of H_2O and HNO_3. After work up, analysis of the compound was done to determine its characteristics. SEM images showed a needle like structure *(Figure 9)* which has a different morphology than the crystals from the first synthesis which might indicate the synthesis was not successful. EDS results showed that the product contained a high amount of Pb. For this reason, the crystals were again put in a mixture of H_2O and HNO_3 to remove the remaining lead parts. During the second washing, the pH of the supernatant changed more as during the previous washing, from 1 to 6. Only a black powder was left after drying the product *(Figure 4b).*

Figure 9. SEM picture of product (II) with ETD detector.

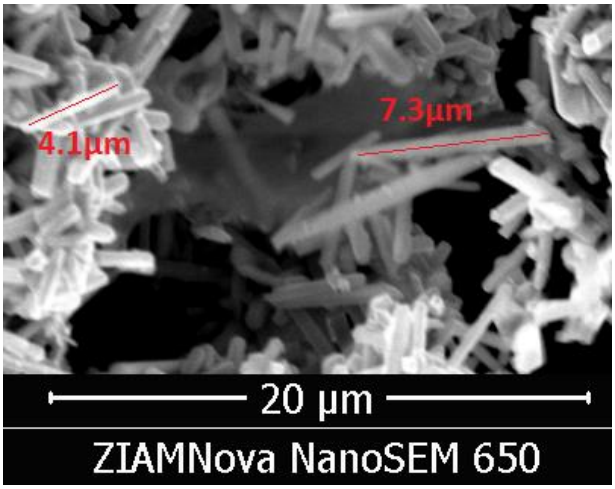

The product was analyzed by PXRD which showed a lot more peaks than expected *(Figure 10a).* The data was then fitted with a diffraction pattern from cryptomelane[32] with the tetragonal space group I4/m in addition to the potassium birnessite diffraction pattern. This was done as a PXRD spectrum recorded by Becerra *et al.*[33] *(Figure 10b)* was a close resemblance to data recorded for potassium birnessite (II). Cryptomelane has chemical formula KMn_8O_{16} with Mn^{2+} and Mn^{4+}. The spectrum of Becerra was obtained after calcinations of $KMnO_4$ at 600°C which is similar to the synthesis of the birnessite. The peaks that were assigned to birnessite by Becerra, are also visible in the data that was collected, however the peaks were too small to determine the content of potassium and water in birnessite. The PXRD spectrum also proved that the synthesis was unsuccessful.

Figure 10. Powder diffraction pattern of potassium birnessite(II) fitted to tetragonal I4/m space group (a). Powder diffraction pattern of birnessite and (b) cryptomelane of Becerra *et al*.[33].

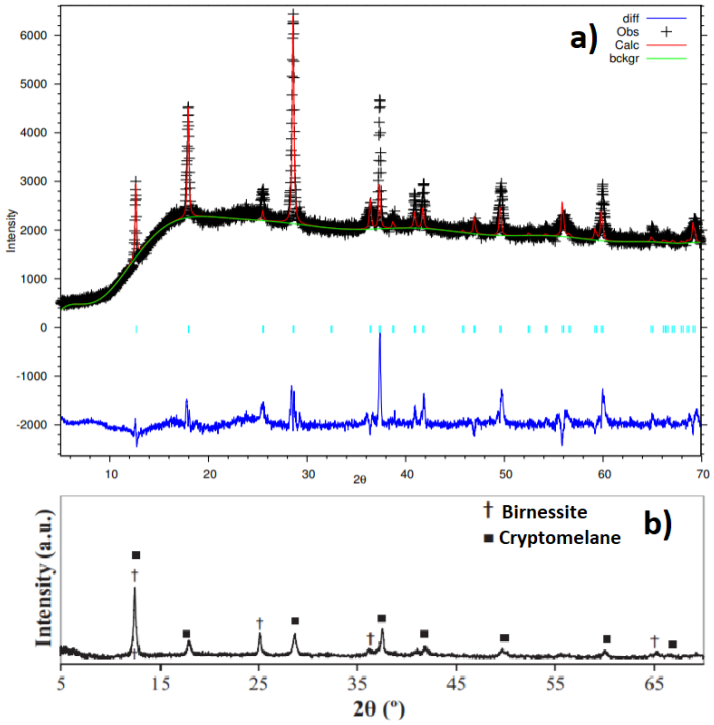

Table 3: Cell parameters after diffraction refinement.

Class	Sgr	a	b	c	α	β	γ
Tetragonal	I4/m	5.1(6)	2.8(4)	7.1(9)	90.(70)	100.(10)	90.(13)

Figure 11. SEM picture of product (II) after 2nd washing with ETD detector.

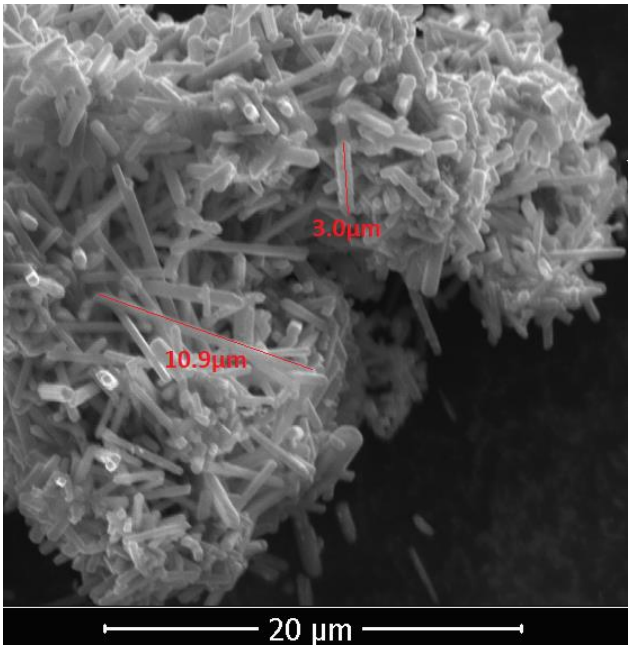

Another picture was taken with SEM *(Figure 11)* after the second washing. The structure of the compound did not seem to have changed very much. Only bigger clusters of needles were visible with needles varying in size from 3-11µm. EDS was also used to see if all the Pb was removed, however, it showed that there was still Pb present in the sample *(Table 4)*. The amount was only slightly reduced after the second washing and thus the contents of the sample most likely were not changed.

Figure 12. EDS spectrum and from *Figure 8.*

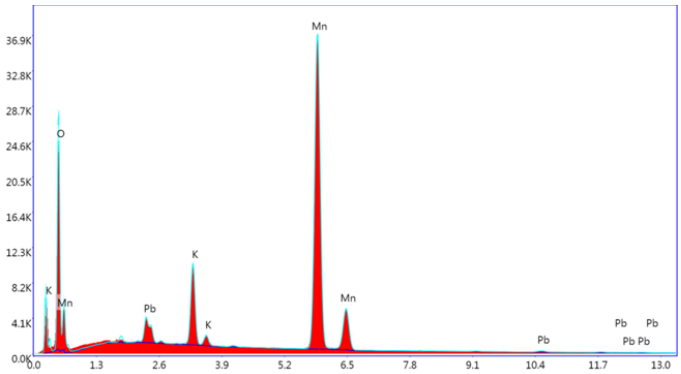

Table 4: Atomic weight percent by EDS-mapping.

Element	Wt%	At%	K_{ratio}	Z	A	F
O K	20.87	47.48	0.0212	1.0412	0.1624	1.0000
PbM	3.47	0.61	0.0187	0.6132	1.3618	1.0909
K K	6.64	6.18	0.0186	0.8821	0.9834	1.0094
MnK	69.03	45.74	0.2138	0.7901	1.0152	1.0052

The amount of K present in the birnessite cannot be calculated by the EDS data as done for potassium birnessite (I), as not all the potassium belongs to birnessite but more to cryptomelane.

Since the data suggests potassium birnessite was not formed, TG-DSC analysis and valance state determination was not performed to determine the stoichiometry.

Conclusion

All data collected after the second synthesis suggests that no potassium birnessite was formed, but rather cryptomelane. The PbO flux used in this synthesis might not be suitable for producing potassium birnessite as the PbO might cause a different reaction to occur than the desired one. Further study is required to see if this is also true when the synthesis is done in an Al_2O_3 crucible, this was not tested due to time constraints.

Potassium Birnessite (III) the third synthesis was performed in an Al_2O_3 crucible as the first two synthesis did not result in de desired products where it be that the crystals were too small or a different product was formed. The water used to wash the crystals was decanted rather

than filtered as it saved time, and was also a suitable method. Figure 4c shows a hexagonal crystal formed with 200µm in diameter which is five times as large as the crystals from potassium birnessite (I). The crystal was still very thin with a thickness of approximately 20µm. The crystals of potassium birnessite (III) were big enough to perform analysis with SCXRD and MPMS.

The SEM pictures confirm that the crystals formed a hexagonal structure *(Figure 13a)*. The layered structure of the crystals can also be observed when the crystals are oriented in a different direction (along the c-axis, *Figure 13b*). The SEM pictures show that the layers are not perfectly aligned but have small defects (the gaps between the layers). The pictures shows crystals with a diameter up to about 300µm and show that the thickness is around 34µm. Along the c-axis it looks like the crystal has layers which range from 2-5µm in thickness.

Figure 13. SEM picture of potassium birnessite (III) with EDT detector show hexagonal layered structure. (a) along the ab-plane and (b) along the c-axis.

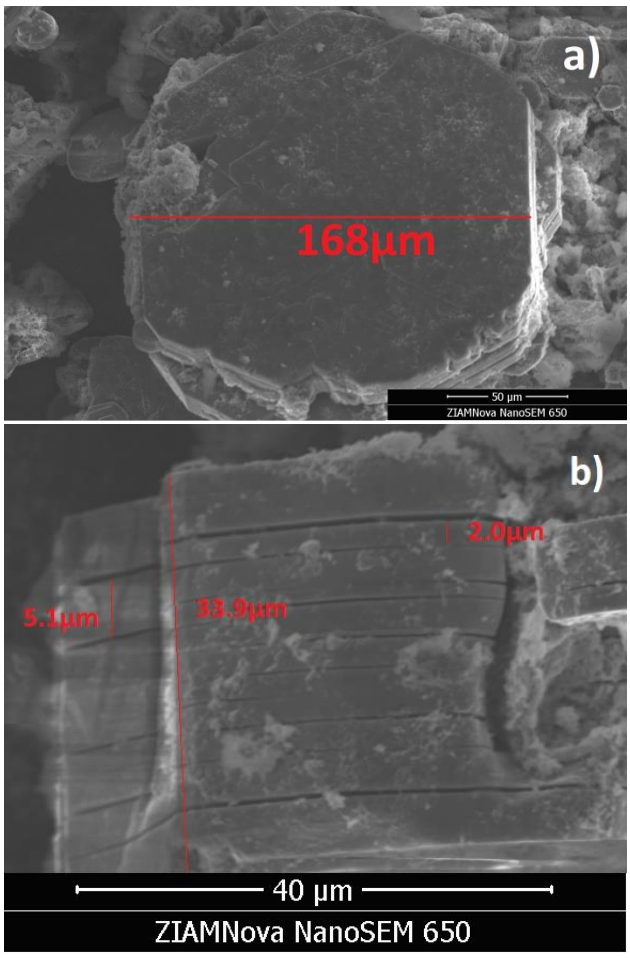

The product obtained by the third synthesis was analyzed by PXRD. However, since the product consisted of crystals it was hard to grind it to a powder since the crystals are very flaky and when they were small, they were quite hard to break. A small peak just above 2θ=50 is observed which most likely belongs to Mn_2O_3 as it is likely that this is also formed during the synthesis of potassium birnessite. There are only two peaks visible of the birnessite due to the difficulty of grinding the crystals as mentioned before. The data shows that just a single phase was present in the sample, as there are not multiple peaks visible at equal 2θ. The powder shows a high preferred orientation in the 00l direction, which made it difficult to fit the spectrum with the right intensities. After refinement of the data, the lattice parameters of the crystals were determined to be as presented in *Table 5*.

Figure 14. Powder diffraction pattern of potassium birnessite(III) fitted to triclinic C-1 space group. ◆ belongs to Mn_2O_3.

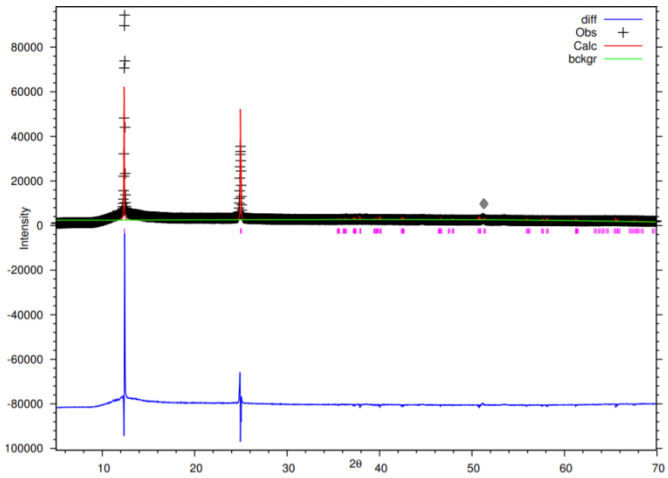

Table 5: Cell parameters after diffraction refinement.

Class	Sgr	a	b	c	α	β	γ
Triclinic	C-1	5.1(1)	2.8(8)	7.2(5)	90.(14)	100.(17)	89.(25)

The positions of the K^+ atoms and H_2O molecules calculated by GSAS were used to attempt to determine structure of the interlayer of the birnessite.

To determine the stoichiometry of the synthesized potassium birnessite first TG-DSC analysis was preformed *(Figure 15)*.The analysis showed three endothermic effects in the sample, similar to that of potassium birnessite (I). They were therefore correlated to the same effects; the loss of surface water, the loss of water embedden in the potassium birnessite structure and the decomposition of birnessite into a manganese oxide respectively. For the first effect, a mass loss of 3.43% was found and the DTG shows that it was completed at 103.9°C with a maximum in the DSC curve at 76.3°C. After the loss of water in the structure the total mass loss was 9.29%. The DTG showed that all water was lost at 186.6°C with a maximum in the DSC curve at 144.3°C. From this, we can conclude that 5.86% water was present in the birnessite. This is more water compared to the

potassium birnessite (I), but still less than shown in previous studies[35]. The decomposition into manganese oxide was finished at 867.8°C according to DTG with a maximum in the DSC curve at 819.9°C.

Figure 15. TG-DSC analysis of potassium birnessite (III). The black and red curve (top) correspond to TG and DSC respectively, while the blue curve (bottom) represents DTG.

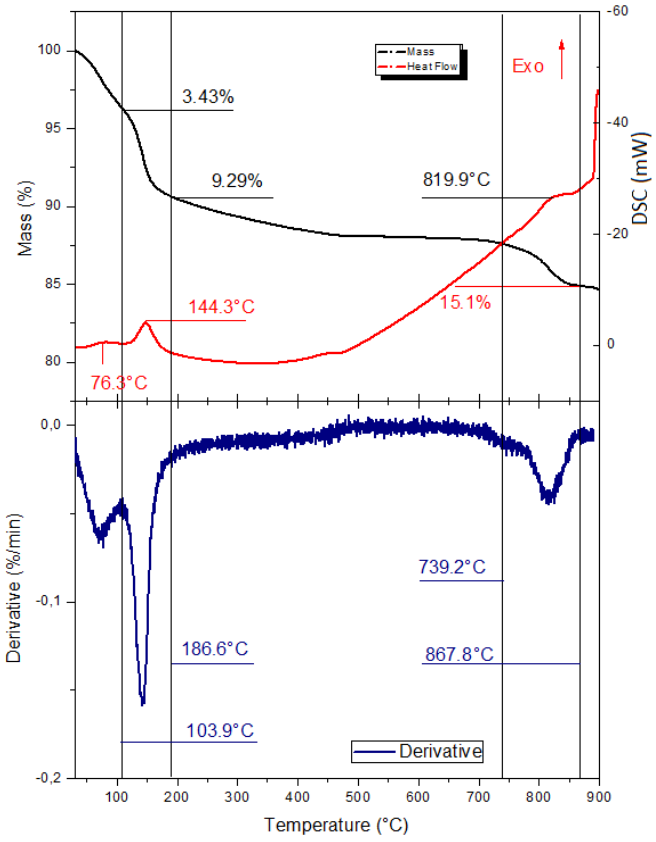

The valence state of this potassium birnessite was determined using the back titration method. Detailed calculations can be found in the appendix. Assuming no oxygen or manganese vacancies, the amount of oxalate used showed the valence state of manganese to be 3.06 this implies that there are almost only Mn^{3+} atoms present in the potassium birnessite and thus almost no Mn^{4+}. Together with the percentage of water obtained from TG, the amount of potassium is determined to be 0.94 and the amount of water is equal to 0.43. This gives us the final chemical formula of $K_{0.94}MnO_2 \cdot 0.43H_2O$.

The SCXRD precession image of the hk0 plane showed interesting behavior. The reflection spots observed showed a splitting in to five different spots. This behavior has been observed in a prior study on potassium-birnessite[26]. This study proposed that the spliting was caused by twinning of the main hexagonal unit cell in two directions giving three spots in one line. The other spots cannot be caused by twinning due to the fact that they have a q-vector diverging at higher angles. Their existence might be explained due to a monoclinic phase. The assignments of the spots can be observed in *Figure 16*. While the PXRD showed that the compound might be triclinic, the SCXRD data suggested a hexagonal or a triclinic unit cell. However, no structure of a triclinic crystal with reasonable positions for K^+ and H_2O could be generated and thus the hexagonal unit cell was chosen.

Figure 16. Enhanced reflection spot of the hk0 precession image. Main hexagonal reflection (yellow), hexagonal twins (green) and monoclinc reflection (blue).

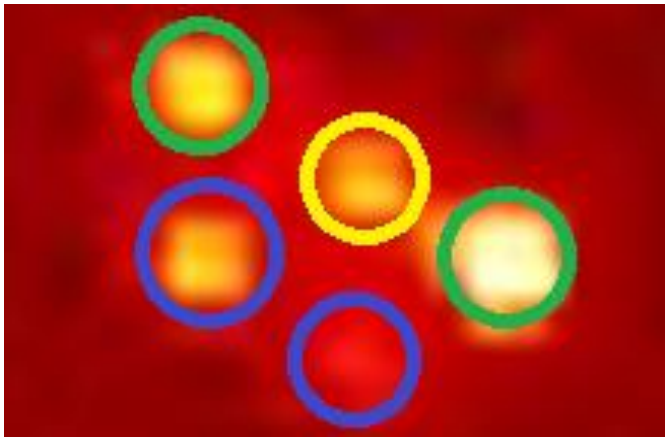

Next to that, the R1 value of the hexagonal structure (0.39) was also lower compared to that of the triclinic structure without the interlayer (0.45) which is preferred to be as low as possible. It should be noted however, that generally an R1 value of less than 0.15 is desired, but due to the splitting and low quality of data a lower value could not be obtained. The structure of the synthesized birnessite can be observed in *Figure 17*. Which shows the

Figure 17. Structure of potassium birnessite.

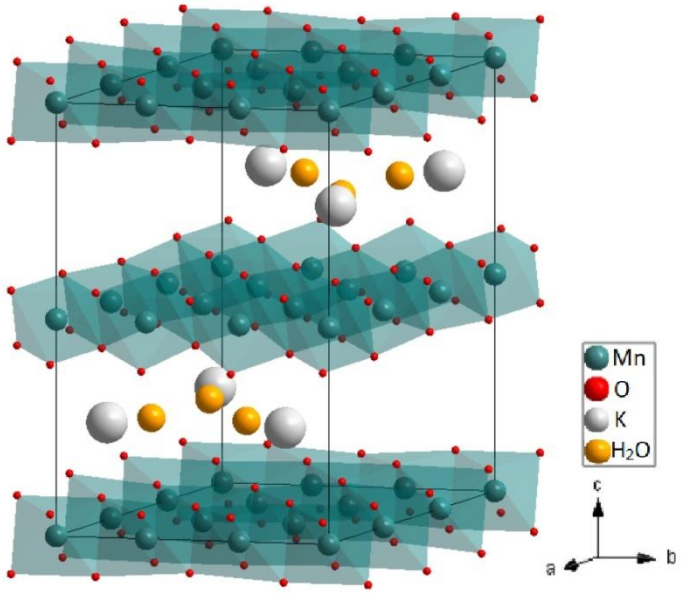

multiple layers as mentioned earlier. However, it should be noted that the coordination of the interlayer of K and H_2O is not fully determined and thus a rough estimation is shown. Also, the occupancy of K^+ could not be calculated by SCXRD and therfore, it was fixed to the results from back titration. The octahedral coordination of manganese and oxygen is observed in the structure which is expected.

Figure 18. Precession image of (a) hk0 plane and (b) h0l plane of potassium-birnessite crystal.

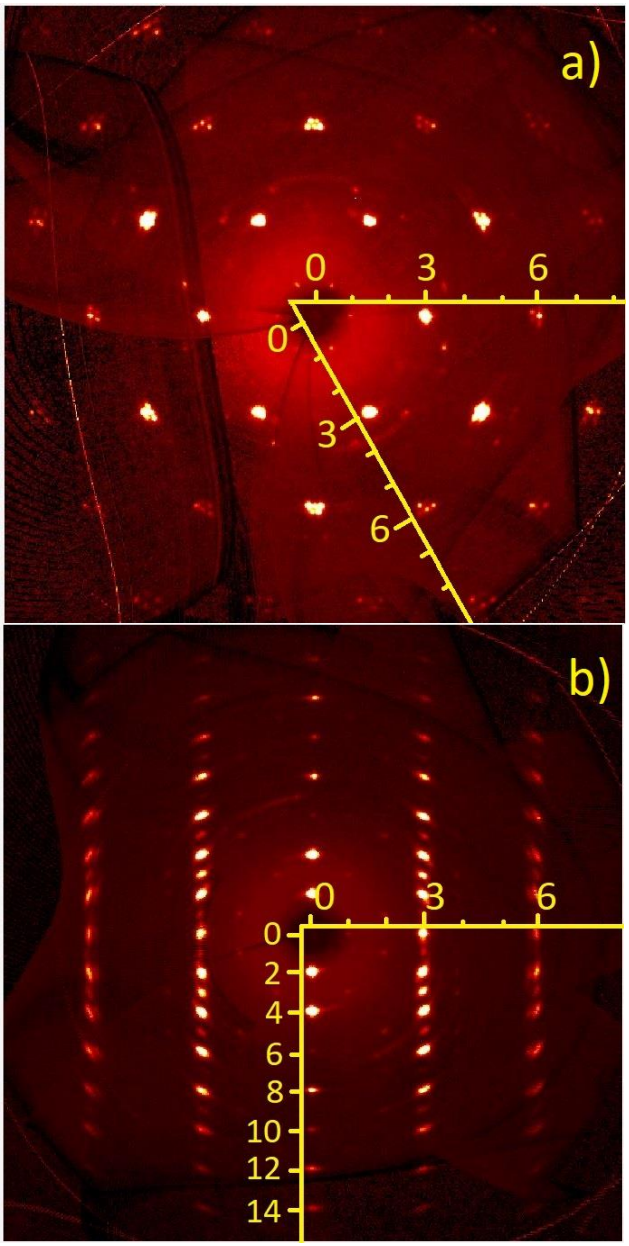

Table 6: Cell parameters from SCXRD

Class	Sgr	a	b	c	α	β	γ	V
Hexagonal	$P6_3/mmc$	8.78	8.78	14.11	90	90	120	942

The *hk0* plane *(Figure 18a)* shows that spots are observed at h & $k = 3n$. The *0kl* and the *h0l* plane *(Figure 18b)* result in similar precession images and therefore, only the *h0l* precession image is shown. It shows spots at $l =$ *even*, which is caused by the c-screw axis present in all $P6_3$ space groups. Furthermore $h = 3n$ is also observed similar as seen in the *hk0* image. From this we can conclude that a hexagonal crystal has been formed.

EDS showed that Al was present in the sample similar to how Pt was present in the first synthesis. Since during this synthesis the largest crystals were grown, it suggests that the material of the crucible influences the crystal growth. More Al was present in birnessite (III) compared to the Pt present in birnessite (I) (1.3 at% compared to 0.1%). This indicates that Al is easier intercalated in the birnessite structure than Pt. It is not accurate to determine the amount of potassium present in the birnessite with *Table 6* (K:Mn 0.27:1) as done for birnessite (I) due to EDS only determining the surface of the crystal. For the first birnessite, it was representative of the amount of potassium due to the small size of the crystals. However, the crystals that were analyzed here were bigger in size and thus the electrons cannot determine the contents of the inside of the sample. Since potassium can decompose at the surface as mentioned before, the actual amount of potassium present is higher than the calculated value for potassium at the surface. Given the fact that potassium can also decompose from the birnessite, the surface likely contains less potassium than the compound.

Figure 19. EDS spectrum and from *Figure 14b.*

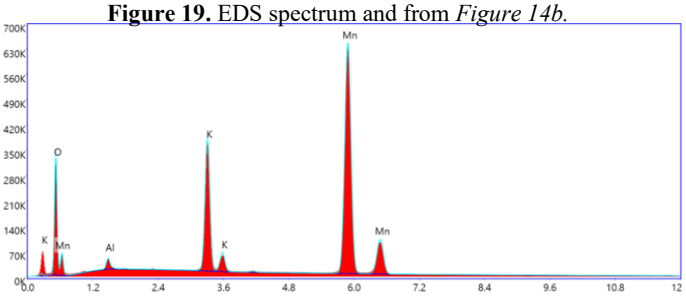

Table 6: Atomic weight percent by EDS-mapping.

Element	Wt%	At%	K_{ratio}	Z	A	F
O K	14.23	34.62	0.0613	1.2296	0.3503	1.0000
AlM	0.93	1.34	0.0047	1.0991	0.4580	1.0023
K K	13.62	13.56	0.1368	1.0453	0.9394	1.0227
MnK	71.23	50.48	0.6627	0.9377	0.9900	1.0023

The DC susceptibility data obtained from the MPMS by applying the magnetic field parallel to the c-axis. The FC and ZFC measurements were measured with an applied field of 5000Oe (*Figure 20*). Transitions were observed for at 49.8°C and 44.1°C for FC and ZFC respectively. It cannot be determined what magnetic structure shift this transition is accounted for. While a splitting is observed between FC and ZFC, the trend of the curves remains similar. This is atypical for potassium birnessite. In a study on Na-birnessite, a splitting is also observed. Here the susceptibility keeps increasing for the

FC measurement and the susceptibility decreases for ZFC after splitting[30]. In the measurement preformed in this study however, the susceptibilities for FC and ZFC both decrease after the splitting resulting in similar values. The observation that the susceptibility rapidly decreases at low temperature might be explained by the theoretical spin network model of dimerised chains[34] or by the theoretical spin network model of the spin ladder[35]. The bigger amount of Mn^{3+} atoms present in the compound promotes the Jahn-Teller distortion[36] which might be capable of destroying the 2D magnetic frustration allowing the 1D spin gap magnetic structure. The data obtained may either be described by the theoretical spin network of the dimer model or that of the spin ladder. This might be concluded as the data obtained by MPMS shows resemblance to the results of Savina *et al.*[37] obtained for β-$TeVO_4$, which suggested a dimer model. The data also shows resemblance to the results from Johnston *et al.*[38] obtained for $(VO)_2P_2O_7$ which suggested a ladder model. Oxygen might be causing the anomaly in the measurements due to the unpaired electrons as it is known to show a transition at around 50K. Because the models are very similar *(Figure 21)*, it cannot be concluded which model is best suited for this case. The Mn_2O_3 phase shows antiferromagnetic ordering, but due to the low amount present the contribution of this to the overall susceptibility is not observed[39]. Further investigation is required to determine the exact magnetic properties of this potassium birnessite. Because of the atypical behavior of the birnessite, a Curie-Weiss temperature (θ_{CW}), an effective moment (m_{eff}), as well as a frustration parameter could not be found for the compound. We can see this by looking at the inverse susceptibility which does not follow the Curie-Weiss law. From this we can conclude that there is some magnetic ordering as the Curie-Weiss law applies only to paramagnetic compounds.

Figure 20. (a) DC susceptibility dependence on temperature and (b) inverse susceptibily dependence on temperature.

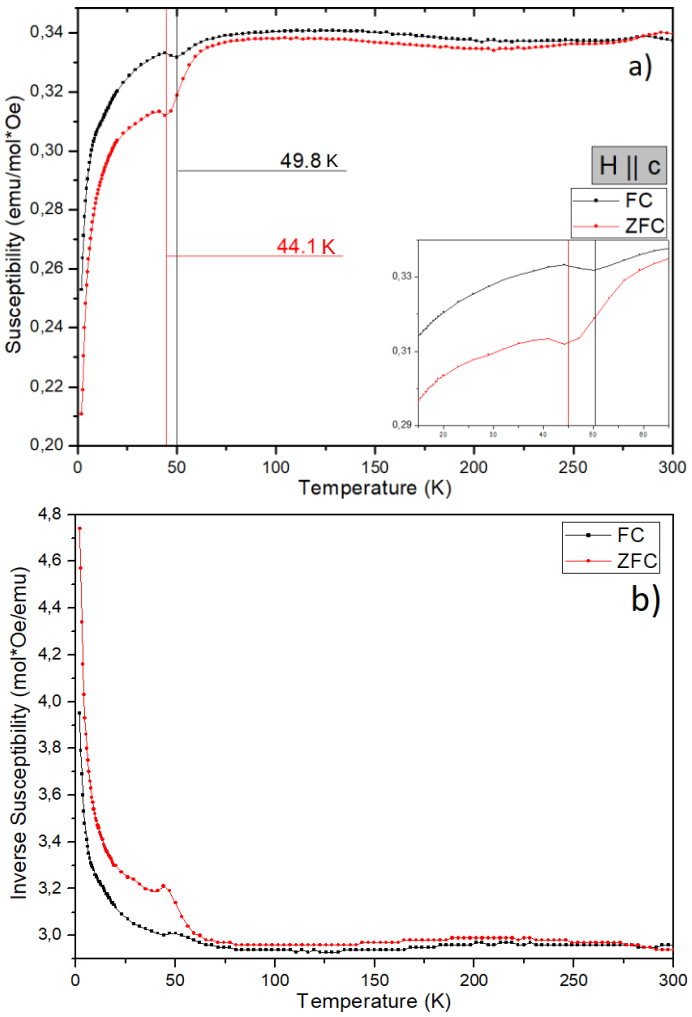

Figure 21. Suceptibility dependence on temperature for theoretical spin arrangements.

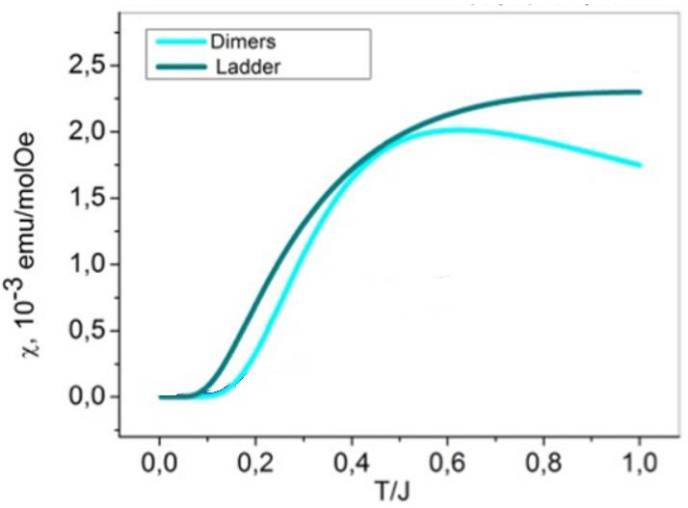

Figure 22. Theoretical spin arrangements for (a) dimerised chain, (b) alternating chainin and (c) spin ladder.

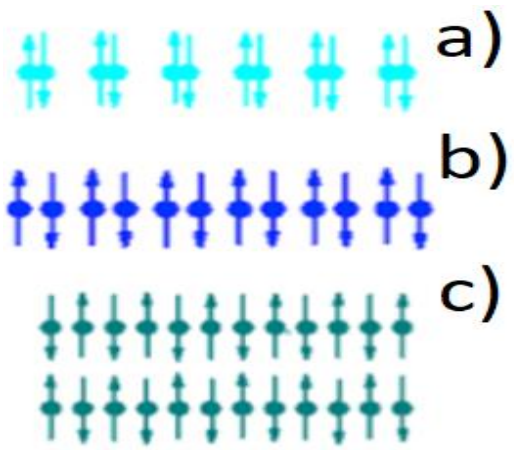

A spin gap may be observed in particular crystalline lattices. Jahn-Teller Some magnetic compounds, allow the formation of antiferromagnetically coupled dimers which cause a spin gap[40,41]. Short ranged spin-spin correlations can lead to a spin gap in the excited spin excitation spectrum between the singlet ground state and the triplet excited state[42]. The spin gap can destroy magnetically ordered ground states at low temperatures despite strong interactions between magnetic units. Theoretical models describe possible arrangements for coupled spin networks (depicted in *Figure 21)* that can cause a spin gap, including a dimerised chain (Bleaney-Bowers[34]), an alternating Chain (Hartfield[43]) and a spin ladder (Troyer-Tsunetsugu-Würtz[35]).

Multiple magnetization vs. applied field scans were performed *(Figure 23)*. The field range was first set from -7T to 7T at 5K. After performing the χ vs T scan, the scan was also performed at 40K and 100K with a field range from -2T to 2T. 5k to obtain data at low temperature, 40K as it was just before the observed transition in *Figure 21* and 100K as the same figure showed that the susceptibility was more or less stable at this temperature. Measurements showed a small hysteresis loops between roughly -0.1T – 0.1T at 40K and 100K and between -0.7T – 0.7T for 5K. The small loop in the data is caused by ferromagnetic contribution, but since the loops are not big, there is only a small ferromagnetic contribution. The ferromagnetic contribution seems to decrease with increasing temperature, as the biggest loop is observed at 5K and the smallest loop is observed at 100K. The magnetization for all measurements at high field shows linear behavior, this is similar to what one would expect for a paramagnetic material. While a magnetic field was applied up till 7T for the measurement at 5K, this was not included in the figure as at 2T the magnetization was already linear.

Figure 23. Magnetization dependence on applied field of potassium birnessite (III) at different temperatures.

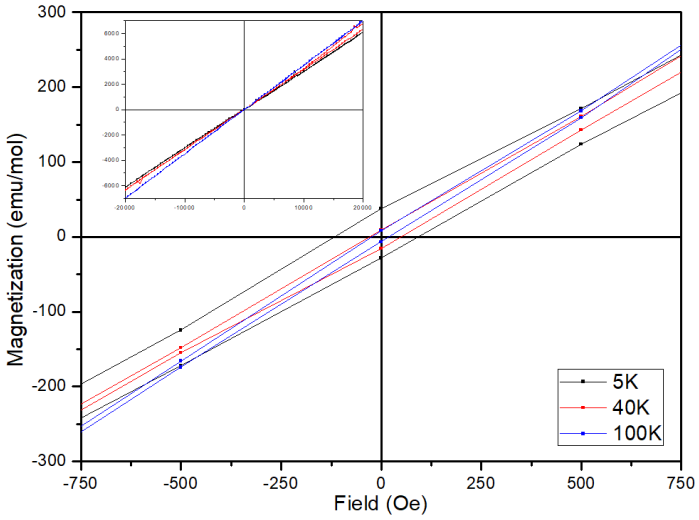

Conclusion

The research performed suggests that running with a PbO and B_2O_3 flux does not result in the synthesis of potassium birnessite but rather in the synthesis of cryptomelane. This was suggested as the PXRD obtained showed a close resemblance to a previous study by Becerra *et al.* [33]. Due to time constraints, the synthesis could not be reproduced and further investigation is required to confirm these hypotheses. It further suggests that an Al_2O_3 crucible is necessary when attempting to synthesize potassium birnessite of the highest quality. This is suggested due to the fact that the only synthesis with crystals big enough to use for SCXRD (up to 300µm) were obtained when using an Al_2O_3 crucible. The collected data suggests that that potassium birnessite crystals were formed with chemical formula $K_{0.94}MnO_2 \cdot 0.43H_2O$ by the third synthesis with only a small impurity of Mn_2O_3 present. SCXRD performed on the crystal showed a splitting which means the structure is probably more complex than presented here but this needs further investigation. SCXRD showed the crystal to be hexagonal with space group $P6_3/mmc$. EDS showed small traces of Al residue from the crucible were present in the crystal further confirming the suggestion that an Al_2O_3 crucible is required for the synthesis of birnessite. The structure showed the expected multilayer system, and octahedral coordination of oxygen with respect to manganese. While the birnessite crystal showed a response to a magnetic field, the observed behavior is peculiar. Due to this odd pattern observed no Curie-Weiss temperature, effective moment and frustration parameter could be found for the compound. The data did not show similarities by previous studies surrounding similar compounds[30] The data suggests a spin gap might be present possibly due to oxygen dimers or a spin ladder. This suggestion comes from the work by Savina *et al.*[37] which data showed similarities with the obtained data. However, this is based purely on theoretical models, and to achieve a full understanding of the magnetic properties more research is required.

Outlook

Since the syntheses were all alterations of each other, the hypotheses proposed can not be fully confirmed. It might for example be possible that a PbO flux together with an Al_2O_3 crucible can result in birnessite formation. A better model for SCXRD to match the data for the splitting in 5 spots is also required to refine the structure better, since the data for only one spot is used in this research. Lastly, the magnetic behavior should be investigated as the compounds that found similar trends in susceptibilty versus temperature and birnessite did not consist out of the same atoms other than oxygen.

References

[1] Wang, L.; Gai, S.; *Contemporary Physics*, **2014**, 2, 75-93.
[2] Kimura, T.; Goto, T.; *et al. Nature*, **2003**, 426, 55.
[3] Abe, N.; Taniguchi, K.; *et al. Phys. Rev. Lett.*, **2007**, 99, 227206.
[4] Tokunaga, Y.; Taguchi, Y.; *et al. Nat. Phys.*, **2012**, 8, 838.
[5] Bos, J. G.; Colin, C. V.; *et al. Phys. Rev. B.*, **2008**, 78, 094416.
[6] Skyrme, T. H. R.; *Nuc. Phys.*, **1962**, 31, 556-569.
[7] Andrikopoulos, D.;Sorée, B.; *De Boeck, J.; J. App. Phys.*, **2016**, 119, 193903.
[8] Jung, J. H.; Matsubara, M.; *et al. Phys. Rev. Lett.*, **2004,** 93, 037403.
[9] Mochizuki, M.; Seki, S. *Phys. Rev. B.*, **2013**, 87, 134403.
[10] Okamura, Y.; Kagawa, F.; *et al. Nat. Comm.*, **2013**, 4, 2391.
[11] Ogawa, N.; Seki, S.; Tokura, Y.; *Sci. Rep*., **2015**, 5, 9552
[12] Okubo, T.; Chung, S.; Kawamura, H.; *Phys. Rev. Lett.*, **2012**, 80, 054416.
[13] Yi, S. D.; Onoda, S.; *et al. Phys. Rev. B.*, **2009**, 88, 195137.
[14] Seki, S.; Mochizuki M.; *Skyrmions in Magnetic materials*, **2015**.
[15] Mühlbauer, S.; Binz, S.; *et al. Science*, **2009**, 323, 915-919.
[16] Castelnovo, C.; Moessner, R.; Sondhi, S. L.; *Nature*, **2008**, 451, 42.
[17] Sampaio, J.; Cros, V.; *et al. Nat. Nanotech.*, **2013**, 8, 839.
[18] Greedan, J.; *J. Mater. Chem.*, **2001**, 11, 37-53.
[19] Toulouse, G.; *Commun. Phys.*, **1977**, 2, 115.
[20] Kijima, T.; *Topics in App. Phys.*, **2001**, 11, 37-53.
[21] Post, J. E.; Veblen, D. R.; *Am. Min.* **1990**, 75, 477-489.
[22] Drits, V. A.; Silvester, E.; *et al. Am. Min.* **1997**, 82, 946-961.
[23] Tseng, L. T.; Lu, Y.; *et al. Sci. Rep.*, **2015**, 5, 9094.
[24] Gaillot, A.; Lanson, B.; *et al. Chem. Mat.*, **2004**, 16, 1890-1905.
[25] Tseng, L. T.;Lu, Y.; *et al. Sci. Rep.*, **2015,** 5, 9094.
[26] Scholtens, R.; Kulish, L.; Blake, G. R.; *Magnetic Frustration: An investigation of Triangular Frustrated Birnessite*, **2019**.
[27] Zhu, Y.; Liang, X.; *et al. Anal. Meth.*, **2017**, vol. 9, 103-109.
[28] Lopano, C. L.; Heaney, P. J.; *et al. Am. Min.*, **2007**, 92, 380-387.
[29] Yang, X.; Tang, W.; *et al. Phys. Rev. B.*, **2016**, vol. 94, 064418.
[30] Kulish, L. D.; Scholtens, R.; Blake, G. R., *Phys. Rev. B., in press.*
[31] Atribak, I.; Bueno-López, A.; *et al. App. Cat. B.*, **2010**, 93, 267.
[32] Vicat, J.; Fanchon, E; *et al. Acta Cryst. B.*, **1986,** 42, 162-167.
[33] Becerra, M.E.; Arias, N.P.; *et al. App. Cat. B.*, **2011**, 260–266.
[34] Bleaney, B.; Bowers, K. D.; *Proc. Roy. Soc.*, **1952**, 214, 451
[35] Troyer, M.; Tsunetsugu, H.; Würtz, D.; *Phys. Rev. B.*,**1994,** 50,
[36] Shen, X. F.; Ding, Y. S.; *et al. J. Am. Chem. Soc.*, **2005,** 127, 6166.
[37] Savina, Y. Bludov, O.; *et al. Phys. Rev. B.*, **2011,** 84, 104447
[38] Johnston, D. C.; Johnson, J. W.; *et al. Phys. Rev. B.*, **1987,** 35, 219.
[39] Grant, R. W.; Geller, S.; *et al. Phys. Rev.*, **1968,** 175, 686.
[40] Whangbo, M. H.; Koo, H. J.; Dai, D.; *J. Sol. State Chem.*, **2003**, 176, 417.
[41] Whangbo, M. H. ; Dai, D.; Koo, H. J.; *Sol. State Sci.*, **2005**, 7, 827.
[42] Manna, S.; Majumder, S.; De, S. K.; *J. Phys. Condens Mat.*, **2009**, 21, 236005.
[43] Hatfield, W. E.; *J. App. Phys.*, **1981**, 52, 1985.13515.

Acknowledgements

First I would like to thank Liliia Kulish for being my daily supervisor and helping me whenever there was some trouble, and learning how all the equipments works. Second, I would like to thank dr. Graeme R. Blake for his supervision and expertise surrounding everything related to crystals and XRD. I would also like to thank Jacob Baas for his technical support. Lastly I would like to thank Joshua Levinsky for his help in analyzing the SCXRD data, and Rick Scholtens for his help surrounding the synthesis of the birnessites.